Intermolecular protein interactions in solutions of calf lens α-crystallin

Results from $1/T_1$ nuclear magnetic relaxation dispersion profiles

S. H. Koenig,* R. D. Brown III,* M. Spiller,* B. Chakrabarti,‡ and A. Pande‡
*IBM T. J. Watson Research Center, Yorktown Heights, New York 10598; and ‡Eye Research Institute, Boston, Massachusetts 02114

ABSTRACT From analyses of the magnetic field dependence of $1/T_1$ (NMRD profiles) of water protons in solutions of calf lens α-crystallin at several concentrations, we find two regimes of solute behavior in both cortical and nuclear preparations. Below ~15% vol/vol protein concentration, the solute molecules appear as compact globular proteins of ~1,350 (cortical) and ~1,700 (nuclear) kD. At higher concentrations, the effective solute particle size increases, reversibly, as evidenced by the appearance of spectra-like ^{14}N peaks in the NMRD profiles and a change in the field and temperature dependence of $1/T_1$. At these higher concentrations, the profiles are very similar to those of calf γ_{II}-crystallin, a crystallin that undergoes an analogous transition near ~15% protein (Koenig, S. H., C. F. Beaulieu, R. D. Brown III, and M. Spiller. 1990. *Biophys. J.* 57:461–469). By comparison with recent analyses of NMRD results for solutions of immobilized proteins as models for the transition from protein solutions to tissue (Koenig, S. H., and R. D. Brown III. 1991. *Prog. NMR Spectr.* 22:487–567), we argue that α-crystallin solute behaves as aggregates $\gtrsim$50,000 kD as protein concentration is progressively increased above 15%. Finally, the concentration dependence of the NMRD profiles of α- and γ_{II}-crystallin can readily explain recent osmotic pressure data, in particular the intersection of the respective pressure curves at ~23% vol/vol (Vérétout, F., and A. Tardieu. 1989. *Eur. Biophys. J.* 17:61–68).

INTRODUCTION

There have been recent suggestions that crystallins, the proteins of eye lens, have evolved unusual associative properties to minimize gradients of osmotic pressure that would otherwise accrue from the gradients of protein concentration in lens (Koenig et al., 1989, 1990; Magid et al., 1989; Vérétout and Tardieu, 1989). Such behavior would be reflected in unusual intermolecular association in crystallin solutions at high concentration since, to first order, osmotic pressure is proportional to the number of solute molecules per unit volume of solution.

Most experimental techniques for studying protein association and oligomerization are of value over a limited range of protein concentration; by contrast, the technique used here is uniformly useful over the range 3–30% protein. We measure the magnetic field dependence of the longitudinal magnetic relaxation rate $1/T_1$ of solvent protons, known as a $1/T_1$ NMRD (nuclear magnetic relaxation dispersion) profile. Diamagnetic globular protein solute induces changes in the NMRD profile of solvent water protons, producing a monotonically decreasing profile with an inflection from which the rotational relaxation time of solute macromolecules, and hence the molecular weight of spherical proteins, can be inferred (Koenig and Schillinger, 1969; Hallenga and Koenig, 1976; Koenig and Brown, 1987, 1991). On the other hand, if the rotational mobility of the protein is restricted (such as can occur upon irreversible heat denaturation or reversibly at high concentration in special cases), a spectra-like set of features (^{14}N peaks), which is known to arise from cross relaxation ("magnetization transfer" of Zeeman energy) between solvent protons and the ^{14}N nuclei of backbone NH moieties (Winter and Kimmich, 1982*a*, *b*; Koenig et al., 1984; Koenig, 1988), appears in the NMRD profile, most visibly between 2 and 3 MHz. The change in the monotonic background is less predictable; what is becoming more clear is that it, too, can have a large component arising from protein–water interfacial magnetization transfer between solvent and solute protons (Koenig et al., 1978; Grad and Bryant, 1990). This contribution depends critically upon whether the solute entities are sufficiently large (rotation appropriately slow) so that solute protons relax as though in the solid state, or sufficiently small so that liquid-state theory is applicable. It depends, further, on the extent to which this behavior is communicated, by magnetization transfer, to solvent protons (Koenig and Brown, 1991).

It was recently shown (Koenig et al., 1990) that there is an unusual dependence of the state of association of calf γ_{II}-crystallin on concentration and temperature. This crystallin begins to oligomerize at relatively low concentrations, the more so the lower the temperature.

M. Spiller's present address is New York Medical College, Departments of Radiology and Neurosurgery, Valhalla, NY 10595.
A. Pande's present address is Boston Biomedical Research Institute, Boston, MA 02114.

0006-3495/92/03/776/10 $2.00

With increasing concentration, oligomerization increases the size of the solute macromolecular entities roughly 10-fold at fixed temperature, to ~300 kD at 15% vol/vol γ_{II}-crystallin and 25°C, at which point a reversible transition occurs that induces ^{14}N peaks at higher concentrations.

In the present paper, we extend the earlier work on γ_{II}-crystallin (Koenig et al., 1990) and lens homogenates (Beaulieu et al., 1988, 1989) to calf cortical and nuclear α-crystallin. We find limited association in solutions of α-crystallin at low concentrations and evidence for very large solute entities at higher concentrations (associated with the appearance of ^{14}N peaks). The molecular weight of α-crystallin, which can depend somewhat on preparation procedures, has been reported at as high as 1,100 (Tardieu et al., 1986). In the present study, we infer somewhat higher, and relatively constant, molecular weights (~1,350 and ~1,700 at 25°C for cortical and nuclear preparations, respectively) in solutions in the range 5–15% vol/vol. At higher concentrations, sufficient solute protein is altered to make ^{14}N peaks visible (Koenig, 1988; Beaulieu et al., 1989). Unlike the case for γ_{II}-crystallin, for which these forms retain sufficient rotational mobility to contribute to the monotonic background of the NMRD profiles as do globular proteins, the α-crystallin particles appear sufficiently large, $\gtrsim 5 \times 10^4$ kD, to be regarded as "microsolids," judging from their slowed rotation. The NMRD profiles become much like those of (irreversibly) immobilized protein (Lindstrom and Koenig, 1974; Bryant et al., 1982, 1991; Beaulieu, 1989; Koenig and Brown, 1991), which, in turn, appear to be models for the NMRD profiles of water protons of most tissue. Indeed, recent ideas on the distinctions between relaxation of water protons in protein solutions and in tissue indicate a transition from liquid- to solid-like behavior for relaxation of the macromolecular protons (Koenig and Brown, 1991) that alters the solvent proton NMRD profiles through magnetization transfer across the protein–water interface. These earlier conjectures are not only enhanced by the results here but, conversely, the present results give added support to the conclusions reached regarding the nature of the changes in solute α-crystallin that set in near 15% protein.

MATERIALS AND METHODS

Calf α-crystallin

Calf α-crystallin from lens cortex (the outer one third by weight) was purified by size-exclusion chromatography at room temperature, using a Sepharose CL-6B (Pharmacia Fine Chemicals, Piscataway, NJ) column as described by McDermott et al. (1988). The α-crystallin from the nuclear region (the inner one third) was prepared in exactly the same manner, and protein eluting in the volume fraction corresponding to cortical α-crystallin was collected. Since the protein from the nuclear region contains a large proportion of so-called high molecular weight (HMW) protein fraction, the α-crystallin fraction thus obtained contained 5–10% HMW. It was therefore rechromatographed in the same column under identical conditions to remove the HMW fraction.

Final crystallin solutions were made in buffers of two different ionic strengths, comparable to those used by Vérétout et al. (1989). The low ionic strength buffer (I = 17 mM) was 10 mM sodium phosphate containing 1 mM EDTA, 0.2 mM DTT, and 0.01% sodium azide at pH 7.0. The high ionic strength buffer (I = 167 mM) contained, in addition, 150 mM sodium chloride.

α-crystallin solutions were concentrated using Filtron stirred-cell concentrators (Pharmacia Fine Chemicals) and Centricon concentrators (Amicon, Beverly, MA) with molecular mass cutoffs of either 10 or 30 kD. Samples were stored at ~18°C; the nuclear preparation turned faintly turbid after 4 d (with no influence on the NMRD data), whereas the cortical preparation remained clear for 1 wk.

The concentrated preparations were diluted as needed by addition of the corresponding buffer solutions. The concentrations of the initial and final solutions, determined optically, were 24 ± 0.2 and 5 ± 0.5% vol/vol, respectively, using an extinction coefficient of $A_{1\,cm}^{0.1\%} = 0.8$.

Measurement and interpretation of NMRD profiles

$1/T_1$ of solvent water protons can be measured at any value of magnetic field over the range 0.01–50 MHz proton Larmor frequency, corresponding to 0.00024–1.2 T, with an automated field-cycling relaxometer developed in our laboratory (Koenig and Brown, 1987). A sample, in a stoppered test tube, is surrounded by circulating freon, allowing measurements in the range −8 to 35°C, with the temperature regulated to within ±0.2°C in order to stabilize the relaxation rates to within the uncertainty of ±0.5% with which they can generally be measured.

Measurements of $1/T_1$ NMRD profiles, which yield the rotational relaxation time τ_R of compact macromolecular solutes, have proven to be particularly useful for studying interactions of diamagnetic globular proteins in solution. Details and references are given in earlier papers of this series (cf. Koenig et al., 1990). In short, the data are fit to the four-parameter Cole–Cole expression (Cole and Cole, 1941) to characterize the monotonic parts of the NMRD profiles, both for the information they contain and for use as a subtractive background so that the structured regions of the profiles can be expanded. Rewritten for $1/T_1$ NMRD data, it becomes (Hallenga and Koenig, 1976)

$$\frac{1}{T_1} = \frac{1}{T_{1w}} + D + A(\upsilon_c)Re\left(\frac{1}{1 + (i\upsilon/\upsilon_c)^{\beta/2}}\right), \qquad (1)$$

where *Re* means "the real part of"; $1/T_{1w}$ is the contribution of solvent; D and A (which is a function of ν_c) are the amplitudes of a high field limiting and a low field dispersive contribution, respectively, to the NMRD profile; and ν is the proton Larmor frequency. The curve has an inflection point (which corresponds to the half-amplitude point of the dispersive component) at

$$\upsilon/\upsilon_c = 1, \qquad (2)$$

and β is a parameter that determines the slope of the profile at the inflection. β = 2 gives a Lorentzian; its value for proton NMRD profiles of most globular proteins is in the range 1.4–1.7 (Hallenga and Koenig, 1976). $1/\nu_c$ is related to τ_R; for spherical proteins (Koenig and Schillinger, 1969; Koenig and Brown, 1991),

$$1/\upsilon_c \simeq 2\pi(\sqrt{3})\tau_R = 10.9\tau_R; \quad \tau_R = 4\pi\eta r^3/3kT, \qquad (3)$$

where r is the radius of the hydrated solute protein, T is the absolute temperature, and η is the (temperature-dependent) microscopic viscosity as experienced by the solute particles. In the dilute limit, $\eta = \eta_0$, the viscosity of the neat solvent, and η/η_0 increases with protein content due to hydrodynamic effects, as discussed by Koenig (1980). The dependence of ν_c on viscosity, temperature, and protein size has been well studied and amply verified (cf. Fig. 2, Koenig and Brown, 1991). The result is ν_c (MHz) $\simeq$ 350/[molecular mass (kD)] at 25°C.

A has an implicit dependence on ν_c; from relaxation theory, the product $A\nu_c$ should have no explicit dependence on ν_c. In addition, the product of ν_c and A per millimole (A_R) is found to be linear in molecular weight (Hallenga and Koenig, 1976; Koenig and Brown, 1991); the relation is (cf. Fig. 4, Koenig and Brown, 1991) $A_R = 9.4 \times 10^{-5} \times$ [molecular mass (kD)]^2. Finally, below ~25% protein by volume, A can be taken to be linear in molar concentration (cf. Koenig et al., 1990) for noninteracting solute molecules; at higher concentrations, effects of one solute molecule on the hydrodynamics of another cannot be neglected.

The utility of the Cole–Cole description for analyzing the $1/T_1$ NMRD profiles of globular protein solutions is that empirical relations among molecular weight, ν_c, and A_R are satisfied by at least one dozen proteins (Koenig and Brown, 1991) ranging over almost three decades in molecular weight; deviations from such behavior are thus indicative of anomalies in protein conformations and interactions. The Cole–Cole expression also provides an excellent description of the NMRD profiles of immobilized protein (Koenig and Brown, 1987, 1991) and tissue (Koenig et al., 1984; Koenig and Brown, 1988), even though the profiles disperse far more slowly than do those of mobile protein. Most of these profiles have similar functional forms (Koenig and Brown, 1991), with $\beta \sim 1$, ν_c near 0.1 MHz and the inflection of the profile rather indistinct (Koenig et al., 1984; unpublished analyses).

RESULTS AND ANALYSES

Data for cortical α-crystallin were taken for low (17 mM) and high (167 mM) ionic strength preparations; no differences were found. Results are reported for only the low ionic strength samples. For α-crystallins, as in all NMRD studies of lens proteins, the effects of concentration and temperature are reversible.

Fig. 1 shows the $1/T_1$ NMRD profiles of a 5% vol/vol solution of cortical α-crystallin, the lowest protein concentration reported here, at three temperatures. The closely spaced data points in the range 1–4 MHz show little evidence of ^{14}N peaks. The solid curves are the Cole–Cole fits (with the 1–4-MHz data left out), with ν_c values indicated by arrows. At 25°C, the value of ν_c = 0.26 MHz corresponds to a mean molecular weight of 1,350, assuming the solute molecules spherical (Koenig

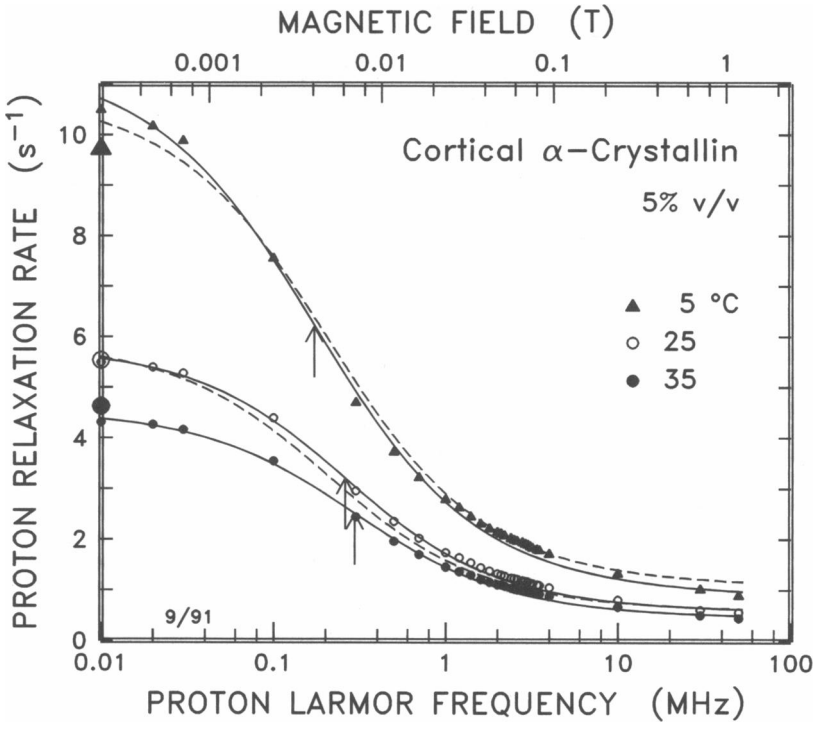

FIGURE 1 $1/T_1$ NMRD profiles of 5% vol/vol calf cortical α-crystallin at 5 (▲), 25 (○), and 35°C (●). The solid curves through the data points derive from a least-squares comparison of the data, excluding the 1–4-MHz region, with the Cole–Cole expression, Eq. 1. The arrows indicate the derived inflection points of the curves, ν_c (cf Table 1). The dashed curves show the profiles expected, relative to the 35°C data, if the variation with temperature could be accounted for only by the expected variation of ν_c, D, and water background with viscosity. $1/T_1$ values at 0.01 MHz for nuclear protein at the same concentration are indicated by large symbols.

and Brown, 1991). The two dashed curves show the profiles expected, relative to the 35°C data, assuming that the observed variation of the profiles with temperature arises only from the variation of solvent viscosity. The good agreement indicates that there is no observable change in either the shape or state of association of the solute molecules with temperature. The profiles of nuclear α-crystallin differ only in minor details (large symbols at 0.01 MHz), with somewhat lower values of ν_c corresponding to 1,700 mean weight and a somewhat reduced variation with temperature. All results of the Cole–Cole analyses are given in Tables 1 and 2. Although the values of the Cole–Cole parameters suggest that, at 5% protein, α-crystallin in solution does not behave as an ideal compact protein, nonetheless this is a very good first-order description.

Fig. 2 shows the $1/T_1$ NMRD profiles, at 25°C, of solutions of five concentrations of cortical α-crystallin. The solid curves derive from the Cole–Cole fit. For 24% protein, were the data point at 0.01 MHz left out, there would be no clear inflection point; thus, the value obtained for ν_c is clearly very sensitive to the accuracy of the 0.01-MHz point. This is true for all the fits for 24% protein, Tables 1 and 2.

The data, Fig. 2, clearly show an onset of peaks, near 2.1 and 2.9 MHz, in the range 15–20% protein. This was previously found for lens homogenates (Beaulieu et al., 1988, 1989) as well as for γ_{II}-crystallin, although the magnitudes of the α-crystallin peaks are not as large and their onset is not as sudden as for γ_{II}-crystallin (Koenig et al., 1990). Also, unlike the behavior of γ_{II}-crystallin, the onset of peaks is not accompanied by a marked increase in the magnitude of the underlying monotonic dispersions.

The data for nuclear α-crystallin are not substantively different from those of the cortical protein, although there is a tendency for the interactions to be somewhat greater (see below) for nuclear than for cortical protein, particularly at concentrations above those at which the peaks appear. The measured rates at 0.01 MHz are shown in large symbols in Fig. 2.

In the absence of a concentration-dependent oligomerization of the protein, ν_c would be independent of concentration at the three lower concentrations (Fig. 2) and decrease somewhat at the higher values because of hydrodynamic effects. This is quantitated in Fig. 3, which shows profiles for nuclear α-crystallin solutions analogous to the cortical data (Fig. 2) but at 35°C. As in Fig. 1, the dashed curves were generated from a profile with ostensibly the least association (5% protein) to indicate the profiles expected if (other than the direct effects of concentration) only the relatively small concentration-dependent hydrodynamic corrections to ν_c were adequate to explain the variation of the profiles, as was done in the earlier study of γ_{II}-crystallin (Koenig et al., 1990).) The results show that, below the concentration for which the ^{14}N peaks appear, this procedure slightly underestimates the magnitudes of the observed profiles, whereas, at higher concentrations, the procedure significantly overestimates A; at 24% protein, the discrepancy is almost a factor of two. It is as though the onset of ^{14}N peaks is accompanied by a (reversible) change of the

TABLE 1 Cole–Cole parameters for cortical α-crystallin

Concentration	Temperature	A	D	β	ν_c
% vol/vol	*°C*	s^{-1}	s^{-1}		*MHz*
24	5	93	0.6	1.16	0.077
	25	56	~0	1.05	0.086
	35	49	~0	0.97	0.074
20	5	66	1.3	1.2	0.101
	25	37	0.7	1.17	0.126
	35	32	0.5	1.10	0.112
15	5	43	0.9	1.26	0.112
	25	24	0.5	1.24	0.149
	35	18	0.6	1.25	0.173
10	5	24	0.67	1.32	0.146
	25	13	0.38	1.33	0.207
	35	9.9	0.34	1.31	0.227
5	5	11	0.39	1.37	0.171
	25	5.3	0.18	1.39	0.257
	35	4.2	0.13	1.39	0.298

A (Which is a function of ν_c) and D, amplitudes of a low field dispersive and a high field limiting contribution, respectively, to the nuclear magnetic relaxation dispersion profile; β, a parameter that determines the slope of the profile at the inflection; ν_c, the inflection frequency.

TABLE 2 Cole–Cole parameters for nuclear α-crystallin

Concentration	Temperature	A	D	β	ν_c
% vol/vol	*°C*	s^{-1}	s^{-1}		*MHz*
24	5	77	0.6	1.17	0.076
	25	50	~0	1.03	0.074
	35	43	~0	0.98	0.075
20	5	62	0.7	1.19	0.085
	25	38	0.2	1.10	0.095
	35	35	~0	1.01	0.076
15	5	40	0.6	1.25	0.104
	25	24	0.3	1.20	0.124
	35	21	0.2	1.15	0.115
10	5	23	0.5	1.28	0.117
	25	14	0.2	1.25	0.141
	35	12	0.2	1.23	0.143
5	5	10	0.29	1.32	0.135
	25	5.6	0.10	1.31	0.177
	35	4.8	0.1	1.27	0.176

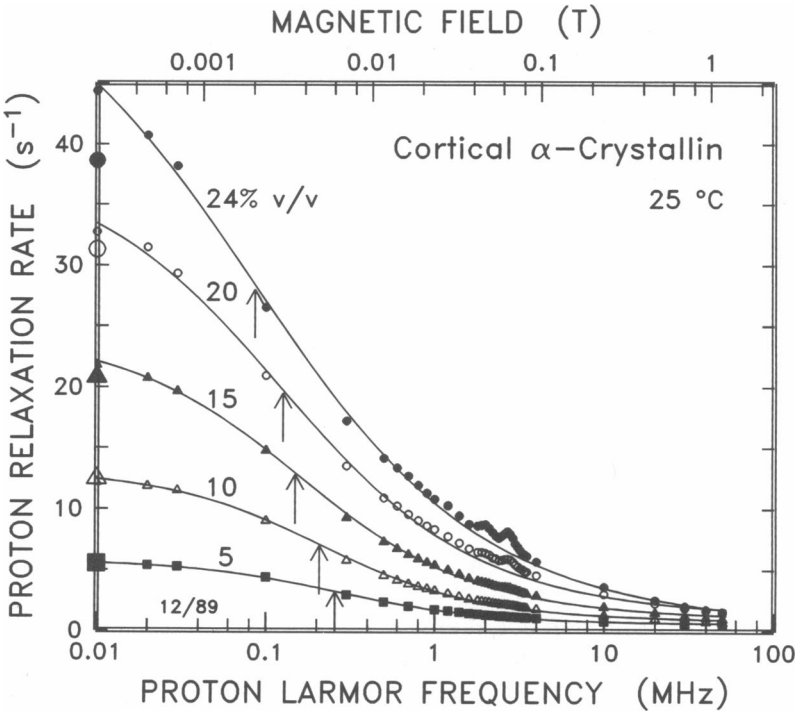

FIGURE 2 $1/T_1$ NMRD profiles of calf cortical α-crystallin, at 25°C, for 24 (●), 20 (○), 15 (▲), 10 (△), and 5% (■), vol/vol. The solid curves through the data points derive from a least-squares comparison of the data, excluding the 1–4-MHz region, with the Cole–Cole expression, Eq. 1. The arrows indicate the derived inflection points of the curves, ν_c (Table 1). $1/T_1$ values at 0.01 MHz for nuclear protein are indicated by large symbols.

relaxation processes that generate the monotonic background. Accompanying this change is a decrease in the value of β (Tables 1 and 2; see below).

Fig. 4 is analogous to Fig. 1, except that the α-crystallin concentration is 24%, the highest used. Two aspects of the α-crystallin data in Fig. 4 differ from the results for 5% protein: (*a*) the dispersion appears much broader (even on a logarithmic plot), expressed in the tables for both cortical and nuclear protein by $\beta \simeq 1$; and (*b*) the three values for ν_c are about equal, with no correlation with temperature. Indeed, the low value of β is about that of most tissues and their model systems, for which the relaxation mechanisms, particularly magnetization transfer, differ in a substantive way from those of solutions of rotationally mobile protein (Koenig and Brown, 1991).

Fig. 5 shows an expansion of the 0.5–4-MHz region of the data of Fig. 4 after (a somewhat imperfect) subtraction of the monotonic backgrounds. Although the spectra are similar in form and magnitude above ~1.5 MHz at the three temperatures, there is structure at lower fields, including a peak near 1.25 MHz, that is most prominent at the lowest temperature. These results also imply, as do the data of Fig. 4, that the conformation of α-crystallin (or distribution of conformers) at high concentration is temperature sensitive. Interestingly, the 5°C spectrum in Fig. 5 is much like those for γ_{II}-crystallin, with a prominent peak near 1.2 MHz (Koenig et al., 1990), whereas the 35°C spectrum (at least for the two main higher field peaks) is much like those of the calf lens homogenate (Beaulieu et al., 1989). A major difference is the near absence of a difference peak near 0.6 MHz (Koenig, 1988) in the present 35°C data, a peak that is strong and isolated in the lens homogenate, and one of a broad grouping in γ_{II}-crystallin.

Fig. 6 shows the magnitude of the major 2.8-MHz peak as a function of protein concentration for six crystallin preparations at 25°C, including data for chicken lens homogenate, for which the secondary structure is mostly α-helical, in contrast to calf lens crystallins, which are predominantly β-sheet. The present data are shown in solid symbols, and analogous data for calf lens homogenate are in corresponding open symbols. The major point to emphasize is that, for all preparations reported to date, the onset of ^{14}N peaks is rather abrupt, their presence becoming distinct above ~17% protein. The peak magnitudes are consistently greater for the calf nuclear than for the cortical homogenates, but more

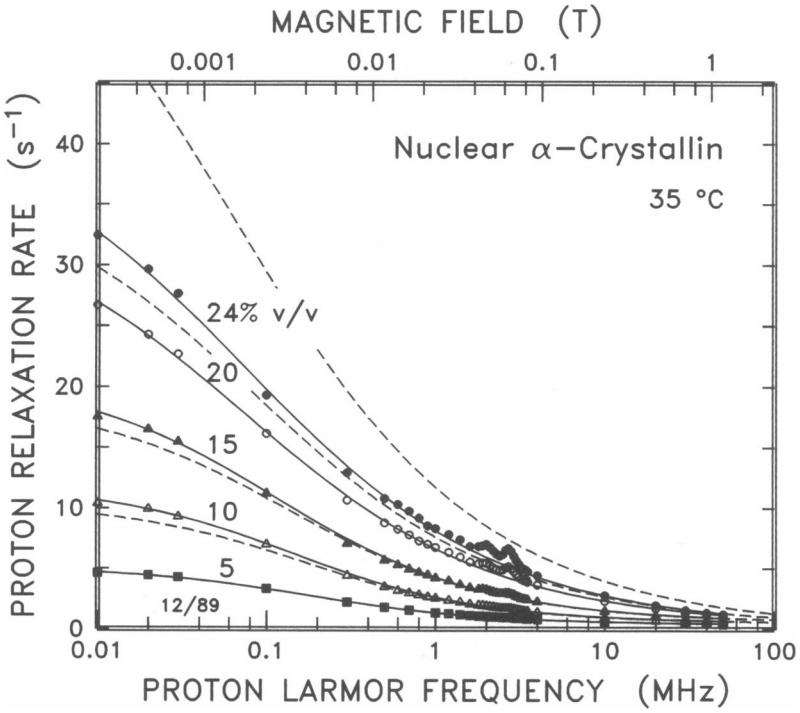

FIGURE 3 $1/T_1$ NMRD profiles of calf nuclear α-crystallin, at 35°C, for 24 (●), 20 (○), 15 (▲), 10 (△), and 5% (■), vol/vol. The solid curves through the data points derive from a least-squares comparison of the data, excluding the 1–4-MHz region, with the Cole–Cole expression, Eq. 1. The dashed curves show the profiles expected, relative to the 5% data, if only concentration-dependent hydrodynamic effects on ν_c are considered.

data would be necessary to discern other systematic variations.

Fig. 7 shows a comparison of the $1/T_1$ profiles of α-crystallin (from Fig. 3) and γ_{II}-crystallin at 35°C for pairs of samples with concentrations ranging from 10 to 24%. Several phenomena are apparent: a much lower molecular weight of solute γ_{II}-crystallin at 10% protein (as estimated from the values of ν_c); its rapid oligomerization; the onset of ^{14}N peaks, slightly different for the two crystallins at this temperature; and the near equivalence of the profiles of both crystallins near 24% protein.

DISCUSSION

Conclusion from α-crystallin NMRD profiles

The major findings here are best summarized by reference to Figs. 2, 3, and 6, which show that the nature of the solute α-crystallin entities changes significantly with protein concentration; the solute particles go from rotationally mobile, relatively unassociated, molecules below ~15% protein to a rapidly increasing fraction of rotationally restricted forms at higher concentrations. Similar behavior, with transitions near 15% protein, was previously reported for calf γ_{II}-crystallin and lens homogenates and for concentrated chicken lens homogenates (which have notably different secondary structures), indicating a general property of crystallins, one relatively insensitive to solvent composition. (No indication of these changes was observed in earlier studies of α- and γ-crystallin [Liang and Chakrabarti, 1982; Siezen and Bindels, 1982; Kono et al., 1990], presumably because of lower protein concentrations and less-sensitive techniques.) It was noted at the time (Koenig et al., 1990) that transition occurs at the solids concentration of blood and most tissues, and it was argued that the rapid association of lens proteins above ~15% vol/vol, which reduces the number density of solute molecules, relates to the need to minimize differentials of osmotic pressure between lens and its surroundings and within the lens itself. Evolutionary pressures for lens transparency have left lens cells without adequate metabolic apparatus to overcome osmotic problems by active pumping; hence the unusual protein–protein interactions of crystallins as a class. This point will not be elaborated further. Rather, what follows are arguments that reinforce the foregoing interpretation of the present data.

These conclusions regarding low and high concentra-

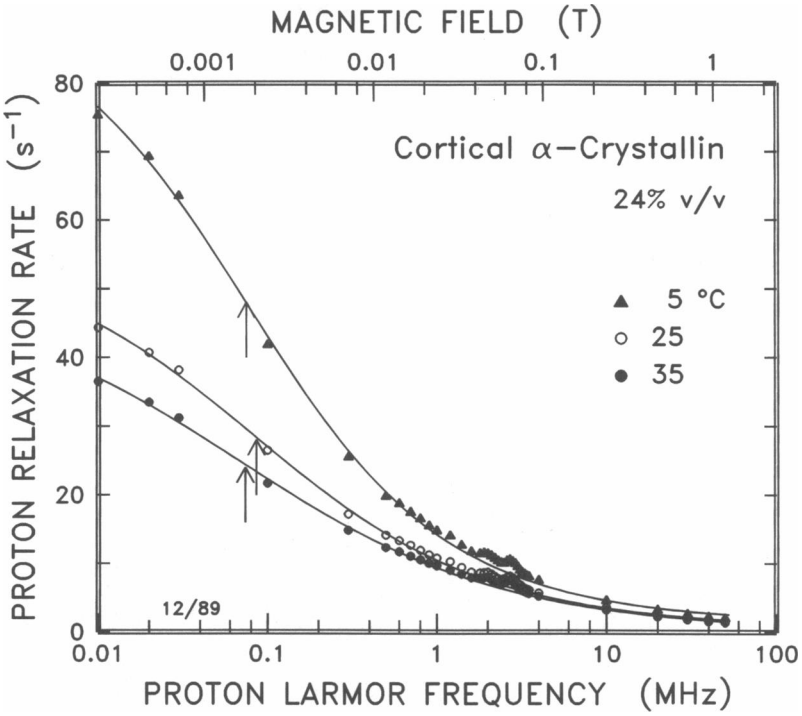

FIGURE 4 $1/T_1$ NMRD profiles of calf 24% vol/vol cortical α-crystallin at 5 (▲), 25 (○), and 35°C (●). The solid curves through the data points derive from a least-squares comparison of the data, excluding the 1–4-MHz region, with the Cole–Cole expression, Eq. 1. The arrows indicate the derived inflection points of the curves, ν_c (cf. Table 1).

tion forms of solute α-crystallin are considerably strengthened on comparison with a wide range of results, many only recently brought together (Koenig and Brown, 1991). Thus, below ~15% protein, the values of A, ν_c, and β (Tables 1 and 2) are sufficiently like those of a wide variety of other proteins with known structures to justify the conclusion that solute cortical and nuclear α-crystallins are well-behaved compact proteins. Their rotational relaxation times correspond to those of spherical proteins of 1,350 and 1,700 kD for the cortical and nuclear preparations, respectively. Moreover, the fact that the relaxation rates in this regime (Fig. 3) increase somewhat faster with concentration than expected shows increasing association with increasing concentration. But these are relatively small effects. However, above ~15% protein, the profiles (Figs. 2 and 3) change in several subtle ways, ostensibly reflecting profound changes in the rotational mobility of the solute molecules. First, rather than the rates increasing rapidly with increasing concentration, they would appear to increase more slowly. Second, β (which measures the slopes of the profiles) decreases rather dramatically, stretching out the dispersive region of the profiles (note that the horizontal scale is logarithmic) and altering their functional forms to those found for immobilized protein and tissue (Koenig and Brown, 1991). In our view, this corresponds to a significant slowing of the rotational relaxation of the protein solute, as well as an alteration in the pathways for relaxation, as we now argue. Moreover, these results have implications for understanding contrast in magnetic resonance imaging (MRI).

Associated with the growth of MRI as a diagnostic tool for clinical medicine has been research on the extent of transfer of magnetization between mobile water and macromolecular protons in tissue (Wolff and Balaban, 1989; Grad et al., 1991) and in what turn out to be excellent model systems: solutions of rotationally immobilized protein (Bryant et al., 1991; Koenig and Brown, 1991). The general results are (*a*) for solutions of proteins $\gtrsim 5 \times 10^4$ kD, whether rotationally mobile or immobile, magnetization transfer dominates the $1/T_1$ NMRD profiles; (*b*) for mobile proteins, $\lesssim 10^4$ kD, relaxation of the protein protons can be described by liquid-state theory (motional narrowing), and relaxation of the transfered magnetization involves only a surface layer of the protein ~5 Å deep; and (*c*) for immobilized protein (e.g., heat-denatured [Beaulieu et al., 1989], cross-linked [Bryant et al., 1991], bound in cells [Koenig and Brown, 1987], and in tissues generally [Koenig and Brown, 1991]), relaxation of the protein protons re-

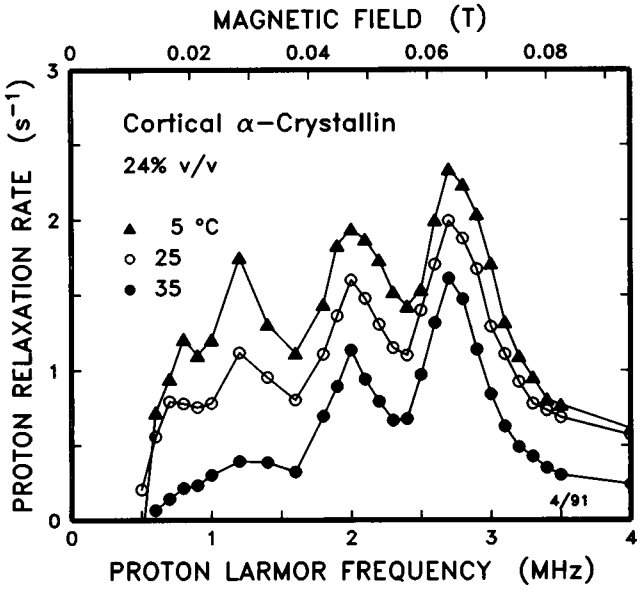

FIGURE 5 The structured regions of Fig. 4, expanded, after subtraction of the monotonic backgrounds, at 5 (▲), 25 (○), and 35°C (●), to illustrate the temperature dependence of the spectral features.

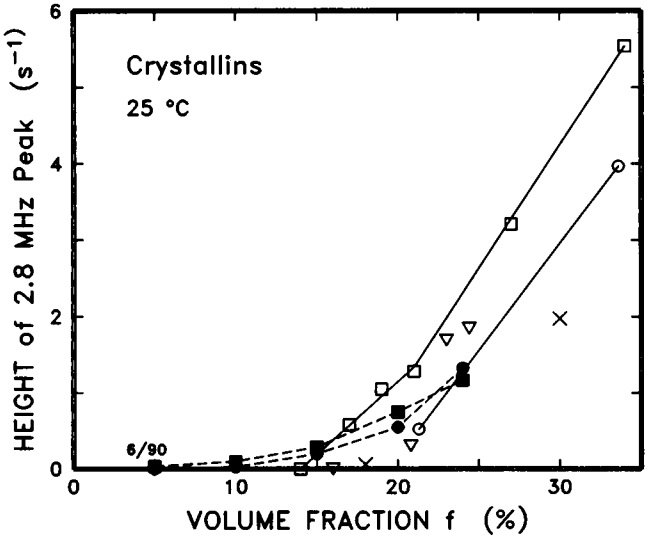

FIGURE 6 The magnitudes of the 2.8-MHz ^{14}N peaks at 25°C, as a function of protein concentration, for calf nuclear (■) and cortical (●) α-crystallin from the present work; calf γ_{II}-crystallin (▽) from Koenig et al. (1990); calf nuclear (□) and cortical (○) homogenates from Beaulieu et al. (1988, 1989); and chicken homogenates (×) from Beaulieu et al. (1989) to illustrate the rather abrupt appearance of the peaks near 17% protein vol/vol in all systems studied. The solid and dashed curves are included as visual guides.

quires solid-state mechanisms for an appropriate description, which involves transfer and diffusion of magnetization to relaxation sinks deep within the macromolecules. As a result, the form of the profiles changes, as does the temperature dependence. In addition (and this has not been remarked on earlier), the high field value of the ratio T_1/T_2 increases dramatically for tissue (cf. Koenig and Brown, 1988) and model systems (Koenig and Brown, unpublished), compared with the predictable behavior of solutions of mobile proteins (cf. Koenig and Brown, 1987). And to further reinforce the circumstantial arguments, Beaulieu (1989) reports anomalously large values of T_1/T_2 for undiluted calf lens homogenates.

Such a transition, from liquid- to solid-like behavior of solute protein, should occur when the rotational correlation time for the magnetic dipolar interaction between neighboring macromolecular protons ($\sim 10^5$ s^{-1}) becomes comparable to the Larmor precession frequency of a proton in the magnetic field produced by its neighbor. One can readily estimate 50,000 kD as an approximate boundary between the two regimes, assuming the proteins spherical. We emphasize that this transition in the nature of the relaxation dynamics of solute proteins is inferred from the NMRD profiles of solvent protons, made apparent through magnetization transfer at the protein–water interface. It is only recently that details of the mechanisms involved have been outlined (Koenig and Brown, 1991).

The present findings for the concentration dependence of $1/T_1$ in solutions of calf α-crystallin, quite similar in all aspects to the behavior of lens homogenates (Beaulieu et al., 1989), mimic the transition from solution to tissue behavior; i.e., they are consistent with a reversible mobile-to-immobile transition, concomitant with the appearance of ^{14}N peaks. The solute entities change from being near 1,000 kD (approximately within a factor of two) at low concentrations (below 15% vol/vol) to solute entities that are solid state–like, from the view of macromolecular protons, i.e., to protein aggregates (assuming sphericity) with molecule weight $\gtrsim 50{,}000$, corresponding to a structural scale of ~ 500 Å. At this stage, we have no way of determining an upper limit to the size of these entities, or even of inferring their shape, except to note that an order of magnitude increase in even a single linear dimension would produce significant light scattering, which is not observed.

The foregoing is consistent with recent work of Morgan et al. (1989), who report two types of ^{13}C high resolution NMR measurements of the protein of bovine lens homogenates. One, that of off-resonance relaxation, is sensitive to the presence of a liquid-like phase; the other, involving carbon–proton interactions, is sensitive to any solid-like phase. They give 35,000 kD as the boundary between their liquid- and solid-like phases, quite in accord with our mobile-to-immobile boundary

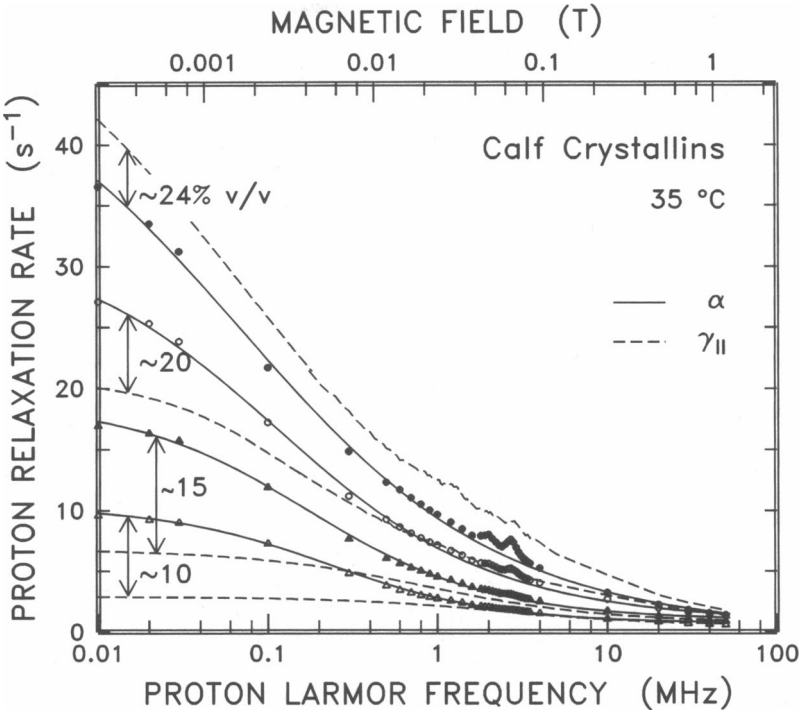

FIGURE 7 Comparison of the $1/T_1$ NMRD profiles of calf γ_{II}-crystallin (*dashed curves*) (Koenig et al., 1990) and cortical α-crystallin (*data points*) at 35°C (from Fig. 3), for pairs of samples with comparable concentrations. The solid curves are Cole–Cole fits to the α-crystallin data, whereas the dashed curves essentially interconnect the published γ_{II}-crystallin data points. For γ_{II}-crystallin, the actual protein concentrations were, from the top, 24.4, 21, 16, and 9.5% vol/vol; for α-crystallin, they were as labeled.

of ~50,000 kD. From quantitation of the resonances of the mobile phase, they infer (but cannot characterize) the presence of an immobilized component in their (high concentration) homogenate. From their measurements of the solid phase, they find comparable amounts of material in the two phases (within a factor of two), with a dependence both on temperature and source of protein (cortical or nuclear). It is gratifying that inferences drawn from the relaxation behavior of ^{13}C nuclei within solute crystallins can be related to the nature of the NMRD profiles of solvent protons, even when the details of the mechanisms of interfacial transfer of magnetization are not yet understood.

Comparison with γ_{II}-crystallin

A cursory summary of earlier conclusions for γ_{II}-crystallin, based on NMRD results (Koenig et al., 1990), is that the ~20-kD monomer oligomerizes with increasing concentration: at 35°C, the effective molecular mass increases from ~30 kD at 3% protein to ~300 kD (approaching the size of α-crystallins) at 15% protein. This was offered as an explanation of the unusual behavior of the osmotic pressure if γ_{II}-crystallin as a function of concentration (cf. Fig. 1 of Vérétout and Tardieu, 1989): its variation is concave downward with increasing concentration, consistent with the number density of solute molecules changing more slowly than the volume fraction. The contrast of the γ_{II}-crystallin profiles with those of α-crystallin is shown in Fig. 7. Compared with α-crystallin, γ_{II}-crystallin below ~15% protein oligomerizes dramatically. At higher concentrations, both crystallins exhibit the behavior evidenced by the appearance of ^{14}N peaks. Near 24% protein, the NMRD profiles of both crystallins are very similar, indicating that the large solute entities, whether α-crystallin or γ_{II}-crystallin, are close to identical in size and shape distributions, including their contribution to magnetization transfer, which, it should be emphasized, depends on the total area of the protein-water interface. Remarkably, the curves that describe the variation of osmotic pressure of α-crystallin and (mixed) γ-crystallin with concentration (Fig. 1, Vérétout and Tardieu, 1989) cross at ~23% vol/vol protein. At higher concentrations, it would appear (both from the osmotic behavior and extrapolation of the NMRD data) that γ_{II}-crystallin solute entities become larger than the α-crystallin aggregates.

This work was supported in part by National Institutes of Health grants T32 EY-07074 (A. Pande) and R01EY-04161 (B. Chakrabarti).

Note added in proof: We have only recently come upon a report of light scattering from solutions of α-crystallin at high concentrations (Andries, C., and J. Clauwaert. 1985. *Biophys. J.* 47:591–605), in which the authors demonstrate the reversible formation of large solute clusters containing ~10^3 molecules of α-crystallin, corresponding to ~750,000 kD. The implications of this for the present work will be considered at a later date; we only note that the amplitudes of both light scattering and NMRD profiles are proportional to molecular weight.

Received for publication 1 July 1991 and in final form 10 October 1991.

REFERENCES

Beaulieu, C. 1989. Nuclear magnetic resonance studies of lens transparency. Ph.D. thesis. University of Michigan Dissertation Information Service, Ann Arbor. 207 pp.

Beaulieu, C. F., J. I. Clark, R. D. Brown III, M. Spiller, and S. H. Koenig. 1988. Relaxometry of calf lens homogenates, including cross-relaxation by crystallin NH groups. *Magn. Reson. Med.* 8:45–57.

Beaulieu, C. F., R. D. Brown III, J. I. Clark, M. Spiller, and S. H. Koenig. 1989. Relaxometry of lens homogenates. II. Temperature dependence and comparison with other proteins. *Magn. Reson. Med.* 10:62–72.

Bryant, R. G., R. D. Brown III, and S. H. Koenig. 1982. Nuclear magnetic relaxation dispersion in monoclinic lysozyme crystals. *Biophys. Chem.* 16:133–137.

Bryant, R. G., D. A. Mendelson, and C. C. Lester. 1991. The magnetic field dependence of proton relaxation in tissues. *Magn. Reson. Med.* 21:117–126.

Cole, K. S., and R. H. Cole. 1941. Dispersion and absorption in dielectrics. I. Alternating current characteristics. *J. Chem. Phys.* 9:341–351.

Grad, J., and R. G. Bryant. 1990. Nuclear magnetic cross-relaxation spectroscopy. *J. Magn. Reson.* 90:1–8.

Grad, J., D. Mendelson, F. Hyder, and R. G. Bryant. 1991. Applications of nuclear magnetic cross-relaxation spectroscopy to tissues. *Magn. Reson. Med.* 17:452–459.

Hallenga, K., and S. H. Koenig. 1976. Protein rotational relaxation as studied by solvent ^1H and ^2H magnetic relaxation. *Biochemistry.* 15:4255–4264.

Koenig, S. H. 1980. The dynamics of water-protein interactions: results from measurements of nuclear magnetic relaxation dispersion. *ACS (Am. Chem. Soc.) Symp. Ser.* 127:157–176.

Koenig, S. H. 1988. Theory of relaxation of mobile water protons by protein NH moieties, with application to rat heart muscle and calf lens homogenates. *Biophys. J.* 53:91–96.

Koenig, S. H., and R. D. Brown III. 1987. Relaxometry of tissue. *In* NMR Spectroscopy of Cells and Organisms. Vol. II. R. K. Gupta, editor. CRC Press, Boca Raton, FL. 75–114.

Koenig, S. H., and R. D. Brown III. 1988. Relaxometry of solvent and tissue protons: diamagnetic contributions. *In* Nuclear Magnetic Resonance Imaging, 2nd ed., Vol II. C. L. Partain, R. R. Price, J. A. Patton, M. V. Kulkarni, and A. E. James, Jr., editors, W. B. Saunders Co., Philadelphia, PA. 1035–1048.

Koenig, S. H., and R. D. Brown III. 1991. Field-cycling relaxometry of proteins and tissue: implications for MRI. 1991. *Prog. NMR Spectr.* 22:487–567.

Koenig, S. H., and W. E. Schillinger. 1969. Nuclear magnetic relaxation dispersion in protein solutions. I. Apotransferrin. *J. Biol. Chem.* 244:3283–3289.

Koenig, S. H., R. G. Bryant, K. Hallenga, and G. S. Jacob. 1978. Magnetic cross-relaxation among protons in protein solutions. *Biochemistry.* 17:4348–4358.

Koenig, S. H., R. D. Brown III, D. Adams, D. Emerson, and C. G. Harrison. 1984. Magnetic field dependence of $1/T_1$ of protons in tissue. *Invest. Radiol.* 19:76–81.

Koenig, S. H., C. F. Beaulieu, R. D. Brown III, and M. Spiller. 1989. Protein-protein interactions, conformation change, and the phase transition in γ_{II}-crystallin solutions. *Invest. Ophthalmol. Visual Sci.* 30:(Suppl.):265. (Abstr.)

Koenig, S. H., C. F. Beaulieu, R. D. Brown III, and M. Spiller. 1990. Oligomerization and conformation change in solutions of calf lens γ_{II}-crystallin. *Biophys. J.* 57:461–469.

Kono, M., A. C. Sen, and B. Chakrabarti. 1990. Thermodynamics of thermal and athermal denaturation of γ-crystallins: changes in conformational stability upon glutathione reaction. *Biochemistry.* 29:464–470.

Liang, J. N., and B. Chakrabarti. 1982. Spectroscopic investigations of bovine lens crystallins. 1. Circular dichroism and intrinsic fluorescence. *Biochemistry.* 21:1847–1852.

Lindstrom, T. R., and S. H. Koenig. 1974. Magnetic-field–dependent water proton spin-lattice relaxation rates of hemoglobin solutions and whole blood. *J. Magn. Reson.* 15:344–353.

Magid, A. D., T. J. McIntosh, and S. A. Simon. 1989. Osmotic pressure of bovine lens crystallins. *Biophys. J.* 55:21*a*. (Abstr.)

McDermott, M. J., M. A. Gawinowicz-Kolks, R. Chiesa, and A. Spector. 1988. The disulfide contents of calf α-crystallin. *Arch. Biochem. Biophys.* 262:609–619.

Morgan, C. F., T. Schleich, G. H. Caines, and P. N. Farnsworth. 1989. Elucidation of intermediate (mobile) and slow (solidlike) protein motions in bovine lens homogenates by carbon-13 NMR spectroscopy. *Biochemistry.* 28:5056–5074.

Siezen, R. J., and J. G. Bindels. 1982. Stepwise dissociation/denaturation and reassociation/renaturation of bovine α-crystallin in urea and guanidine hydrochloride: sedimentation, fluorescence, near ultraviolet and far ultraviolet circular dichroism studies. *Exp. Eye Res.* 34:969–983.

Tardieu, A., D. Laporte, P. Licinio, B. Krop, and M. Delaye. 1986. Calf lens α-crystallin quaternary structure. A three-layer tetrahedral model. *J. Mol. Biol.* 192:711–724.

Vérétout, F., and Tardieu. 1989. The protein concentration gradient within eye lens might originate from constant osmotic pressure coupled to differential interactive properties of the protein. *Eur. Biophys. J.* 17:61–68.

Vérétout, F., M. Delaye, and A. Tardieu. 1989. Molecular basis of eye lens transparency. Osmotic pressure and X-ray analysis of α-crystallin solutions. *J. Mol. Biol.* 205:713–728.

Winter, F., and R. Kimmich. 1982*a*. Spin lattice relaxation of dipole nuclei (I = ½) coupled to quadrupole nuclei (S = 1). *Mol. Physiol.* 45:33–49.

Winter, F., and R. Kimmich. 1982*b*. NMR field-cycling relaxation spectroscopy of bovine serum albumin, muscle tissue, *micrococcus luteus,* and yeast. $^{14}N^1H$ quadrupole dips. *Biochim. Biophys. Acta.* 719:292–298.

Wolff, S. D., and R. S. Balaban. 1989. Magnetization transfer contrast (MTC) and tissue water proton relaxation *in vivo. Magn. Reson. Med.* 10:135–144.